

AN IMAGE-BASED METHOD TO CLASSIFY POWER LINES IN LIDAR POINT CLOUDS

Sebastián Ortega

Institute of Applied Microelectronics
Universidad de Las Palmas de Gran Canaria
sebastian.ortegatrujillo@gmail.com

Agustín Trujillo

José Miguel Santana
Imaging Technology Center
Universidad de Las Palmas de Gran Canaria
{agustin.trujillo , josemiguel.santana}@ulpgc.es

José Pablo Suárez

Institute of Applied Microelectronics
Universidad de Las Palmas de Gran Canaria
josepablo.suarez@ulpgc.es

ABSTRACT

Power line management becomes critical as power companies need to assure the reliability of their services. Many of them rely on LiDAR scanning of their assets to get information about the status of the power line corridor and possible dangers in the area. In this paper, a novel method to classify wire and pylon points from a LiDAR point cloud is introduced. The method generates images from different measurements of the data to select candidate areas and then applies a clustering algorithm to group and filter out false positives. A prior classification of ground points is not necessary for the method to work. Tests have been conducted on a set with 25 point cloud files to show the effectiveness of the presented method.

KEYWORDS

Power lines, point clouds, classification, clustering.

1. INTRODUCTION

The management of power lines is an issue of special importance for power companies due to the needs of ensuring a continuous service to a population whose dependence on energy is always increasing. Service could be interrupted due to damages caused by the fall of objects, generally trees, over the power line. Moreover, forest fires could start as a result of these events, producing another kind of inconveniences on the people.

During the last years, the use of *Light Detection and Ranging* (LiDAR) becomes frequent in power line management. It refers to a kind of active sensor which determines the distance between its laser emisor and the ground or an object. [1]. LiDAR devices can be differenced in two categories: waveform sensors, which offer the whole laser return, and discrete sensors, which capture only a certain number of returns. This number varies depending on the device: most models provide between 3 and 5 returns.

Generally, LiDAR data is presented as *point clouds*. Every point includes, at least, accurate X-Y-Z values, an intensity value and its associate return number. Some sensors also add extra information about each point, like RGB color values. A frequently used format to represent these point clouds is the *Laser File Format* (LAS), whose specifications can be found in [2].

In this work, a new method for the classification of power structures in discrete LiDAR point clouds is presented. The method classifies the points of interest into two categories: pylon and wire. The structure of the document is as follows:

Firstly, an analysis of the data is conducted in Section 2. After that, the applied method to perform classification is explained in Section 3. Section 4 introduces the experimentation which has been conducted to fit the parameters of the method and

validate its behaviour. Finally, the conclusions of this work are presented in Section 5.

1.1. Related work

A great amount of previous works deal with classification of LiDAR points applied to a wide variety of topics. As an example, it is used in [3] for the classification of different elements in a complex natural scene, like rives, cliffs, rocks, etc. Antonarakis et al. [4] introduced a method to efficiently classify ground and forest points. Dalponte et al. [5] combined LiDAR with hyperspectral data to classify complex forest scenes. The work of Omar et al. [6], in which different kinds of aerosols are classified, is also highlighted.

However, the two areas in which there is a greater number of papers are the urban scene and the power line classification. Some examples on the use of point classification in urban scenes are the work of Niemeyer et al [7], where a *Random Forest* (RF) classifier is integrated on the CRF framework to detect buildings in a point cloud. Yao et al. [8] developed a segmentation method to extract vehicles in a urban scene. Moreover, Man et al. [9] explored the efficiency of pixel-based and object-based classifiers in a urban scene which includes LiDAR and hyperspectral data.

For the case of power lines there also exists a wide range of studies. Liu et al. [10] applied the Hough transform on a subset of the point cloud after conducting an analysis on skewness and kurtosis of the data. Jwa et al. [11] introduced the *Voxel-based Piecewise Line Detector* method. Kim and Sohn used a RF classifier to identify 5 classes of points, including wire and pylon [12], and then integrated it into a *Multiple Classifier System* [13]. Zhu and Hyypä [14] introduced an algorithm which uses height data to identify low-voltage lines in forested areas. Liang et al. [15] studied the orientation of the power line and then grouped candidate points in single lines. Finally, Ritter and Bengler [16] used tensor fields and eigenvectors to reconstruct the line. Many other works can also be found in an extensive survey done by Matikainen et al. [17].

Most of the cited works required a previous stage in which ground-related points are removed with other algorithms [10, 12, 13, 15]. Those which do not require it are focused only in classification of wire points [11, 14, 16]. Our contribution is an alternative method which allows the classification of wire and

pylon points without an initial classification of ground points.

2. STUDIED DATASET

For this study we have worked over 68 point cloud files, which contain between 1.5 and 2.5 million points per file and an average point density per square meter of 25.5. The files represent an helicopter-based scanning of power lines across 80 km. of an electric power line. Data include power line points as well as points representing terrain, all kinds of vegetation, buildings, roads and water masses. The files have been divided into three different sets:

Training set (20 files): Used to conduct previous analyses on the data.

Validation set (23 files): Used as a sandbox to adjust the parameters.

Test set (25 files): Used to conduct the experimentation and obtain the final results.

2.1. Data Analysis

Prior to the development of any method, it is important to analyze the available data to find what makes all the possible elements in the point cloud different from each other. The focus is put on the three variables that are included in the minimum version of LAS point clouds: height, intensity and return value.

The height value can be used in terms of distance between the point and the underlying ground to determine where a power line could be found. Power lines are supported by pylons with diverse shapes and heights. Most pylons for high voltage lines have heights between 10 and 55 meters [18]. That also implies that wires can be found at heights of at least 8 meters.

	Terrain	Vegetation	Buildings	Pylons	Wires
<i>Min</i>	35	37	44	35	0
<i>Max</i>	5843	5843	4774	4819	4752
<i>Mean</i>	3070	2995	2415	2050	1370
<i>Std</i>	91.12	203.8	506.9	60.56	34.88

Table 1 Resume of intensity data analysis

To find conclusions from the intensity of the return, maximum, minimum and mean intensity values have been extracted from the twenty files of the training set. The results are presented here as a resume in Table 1.

**Sebastián Ortega, Agustín Trujillo,
José Miguel Santana, José Pablo Suárez**

From the analysis of the set can be extracted that all categories present similar minimum and maximum values, meaning that the category of a single point cannot be inferred from its intensity information. However, mean and standard deviation for the whole set of category points allow to make some differentiation. Particularly, groups for power line components have lower and less diverse returns than the rest of the categories. As an example, the ratio of intensities between the mean for wires and the global maximum is 0.23. For the case of pylons, the same ratio has a value of 0.34. This fact enables us to differentiate the two categories based on the mean intensity value of the cluster.

The third variable, the return number, cannot be applied to single points either. However, it is expected that in regions with more than a possible return, the nearest point has a minor return value. Moreover, high human-made objects (like pylons or buildings) are expected to have a face full of 1st return points and other one with more points obtained from last returns, since the LiDAR device will be opposed only to a given side of the object. An analysis on the distribution of returns for the training set has been performed, and its resume can be read in Table 2:

	Terrain	Vegetation	Buildings	Pylons	Wires
1 - M	82.66%	80.76%	75.07%	67.75%	90.63%
1 - S	5.78	6.83	26.82	5.20	5.74
2 - M	14.75%	16.42%	14.13%	26.80%	8.59%
2 - S	4.11	5.08	6.35	2.42	4.46
3 - M	2.22%	2.46%	2.65%	5.23%	0.69%
3 - S	1.46	1.53	4.55	2.27	1.18
4 - M	0.32%	0.31%	2.96%	0.70%	0.07%
4 - S	0.26	0.25	8.88	0.80	0.17
5 - M	0.04%	0.03%	2.90%	0.08%	0.01%
5 - S	0.04	0.03	9.13	0.15	0.02

Table 2 Return distributions per category. First column expresses the return number and a M (mean) or S (standard deviation).

From the resume can be extracted that, for the pylon category, standard deviations from the mean of 1st and 2nd returns are lower than in the rest of the groups. The percentage of first return points are quite low compared with the same percentage in other categories. These facts can be used to filter clusters of points that represent pylons.

Other remarkable fact is a high percentage of first return points in the wire category. Combined with the

information about height and intensity, this could help identify clusters of points as wires.

3. METHODOLOGY

In this work we propose a pipeline to classify accurately the power lines from the LiDAR data. It applies two stages: an initial stage which performs an image-based selection of candidate areas, and a final stage which filters these areas to remove possible false positives. Both stages are presented in detail in the following subsections.

3.1. Image-based classification

This stage proposes the generation of images in which every pixel represents a squared volume whose section side has α meters length. The generated image should cover the whole point cloud regardless of the number of points in each pixel. The goal of those images is to separately differentiate wire and pylon areas of the electric power line from the rest of elements in the point cloud. To do so, different measurement images should be created from the available data, in this case, intensity and height values, and then combined.

One of these measurement images is the minimum height, H . There, every pixel H_{ij} is assigned the minimum height from the points contained in the $[X_{min} + (i-1)*\alpha + 1, X_{min} + i*\alpha ; Y_{min} + (j-1)*\alpha + 1, Y_{min} + j*\alpha]$ XY region of the point cloud, from now on, its *associate volume section*. There, X_{min} and Y_{min} stands for the minimum X and Y values for the point cloud.

By using H , it is possible to compute an image of amplitude, A . Every pixel A_{ij} of the image is assigned the result of the Expression 1:

$$A_{ij} = \sum_{k=1}^n (Z_{ijk} - H_{ij}) \quad (1)$$

Where Z_{ijk} stands for the height value of every point in the associated volume of the pixel (i,j). Therefore, A is an accumulator of height differences. In case no points are present in the volume, H_{ij} and A_{ij} are assigned the global minimum height and 0, respectively. Finally, A is normalized within the range [0,1].

Having A , we can define a binary image, T , which signals the presence of power line pylons. The assignation of T_{ij} follows the rule:

$$T_{ij} = 1 \text{ if } A_{ij} \geq \gamma$$

$$T_{ij} = 0 \text{ otherwise.}$$

There, γ is an adjustable threshold which should be assigned in a way that allows the detection of the maximum number of pylon points with the minimum possible number of false positives. Experimentation was conducted and introduced in Section 4 to find a proper value for the parameter, which was finally assigned 0.25. Examples of T images can be seen on Figure 1.

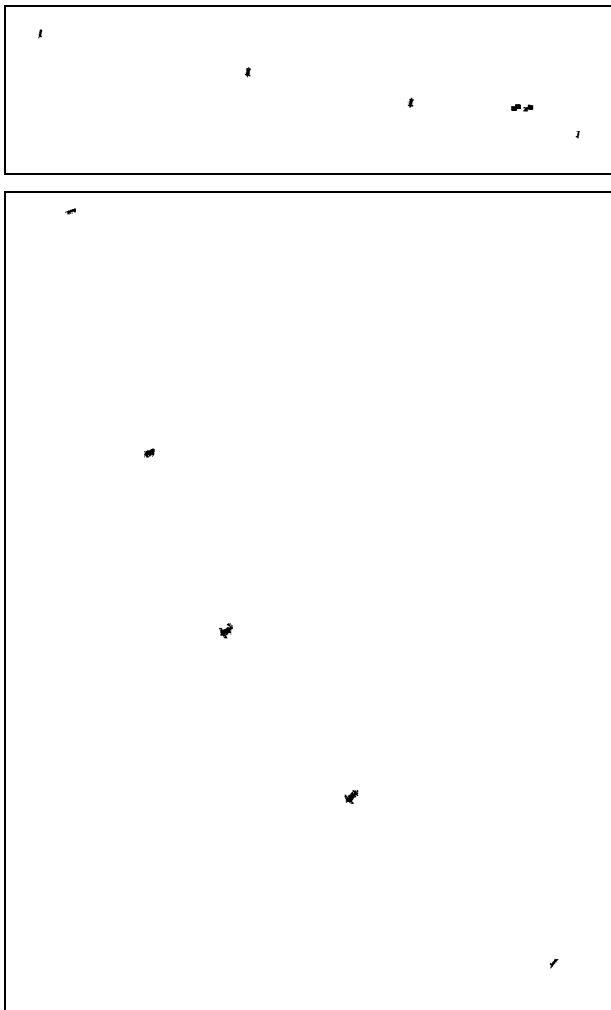


Figure 1 Inversed T images for two files of the validation set.

Other measure images are based on intensity values. Let ε be the minimum possible height value for a wire point in relation with the ground height below it. Considering this, we define an intensity accumulate image, I' , whose pixel values are assigned using the Expression 2:

$$I'_{ij} = \sum_{k=1}^n I_{ijk} \cdot Q_k \quad (2)$$

Where I_{ijk} is the intensity value of the points in the associate volume of the pixel, and Q_k is a binary

evaluation for each point whose value is given by the following rule:

$$Q_k = 1 \text{ if } (Z_{ijk} - H_{ij}) > \varepsilon$$

$$Q_k = 0 \text{ otherwise.}$$

Other image, N , is defined and their pixels assigned the number of points included in their associated volumes which fulfills $Q_k = 1$. This way, we can define a mean intensity image, M , assigning their pixels as in Expression 3:

$$M_{ij} = \frac{I'_{ij}}{N_{ij}} \quad (3)$$

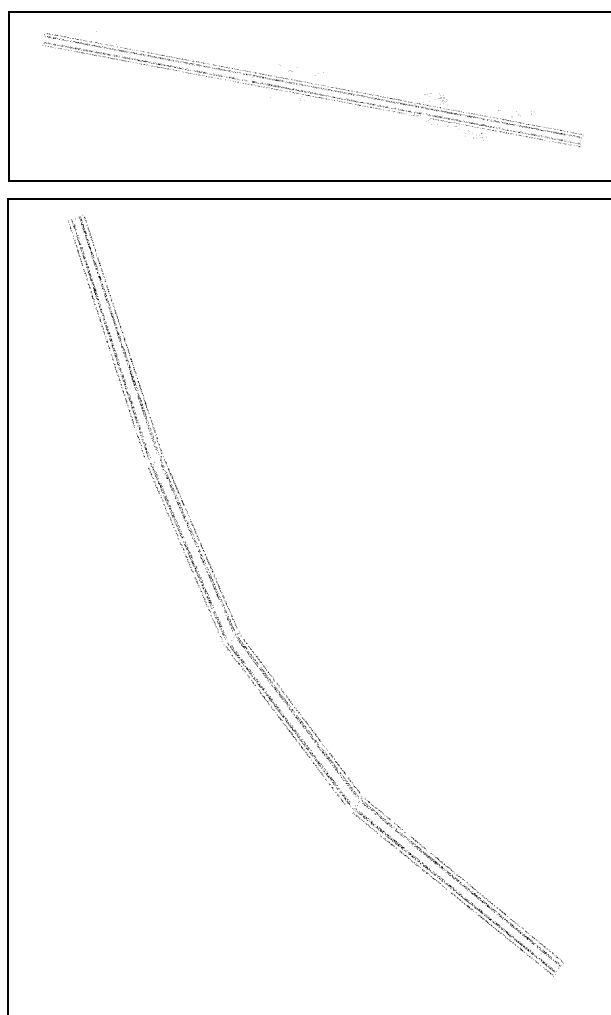


Figure 2 Inversed W images for two files of the validation set.

M is then adjusted so its values range between 0 and 1. Having M , the binary image W which signals the presence of wires surges from the rule:

$$W_{ij} = 1 \text{ if } M_{ij} < \omega \text{ and } T_{ij} == 0$$

$$W_{ij} = 0 \text{ otherwise}$$

The ω parameter is used to filter regions with low mean intensities. A low intensity in LiDAR data implies a low reflectivity, only seen in objects as power lines, pylons or dense vegetation areas. Considering the intensity ratios commented in Section 2.1, we decided to set this value to 0.3, which is an intermediate value between the wire average (0.23) and the pylon average (0.34), suppressing the latter. Figure 2 shows some examples of wire images.

An initial classification of points is performed from T and W images, classifying as pylons all points whose associated pixel in T is selected, and as wires those points whose associated pixel in W is selected and have a height difference with the ground greater than ϵ .

3.2. Filtering selected areas

The initial classification provided by the first stage of the pipeline can include false positives, generally due to high vegetation with similar intensity values or placed immediately below the wire, as seen in Figure 3. This filtering stage aims to remove those false selections by using the return number of the points and their intensity.

The pylon case can be dispatched by checking the distribution of return values in the candidate area. As shown in the data analysis from Section 2.1, points grouped under the pylon category show a distribution of return values with low percentages in the first return and low deviations. It could happen that the candidate cluster contains some wire or terrain points near the pylon itself, so the conditions should be slightly less restrictive than the ones suggested by the analysis. We are considering a candidate area as a pylon if it fulfills all the following criteria:

- First return points: $> 63\%$ of the points.
- Second return points: between 19% and 30%
- Third return points: between 2% and 6.5%

Mean intensity value: below 2200

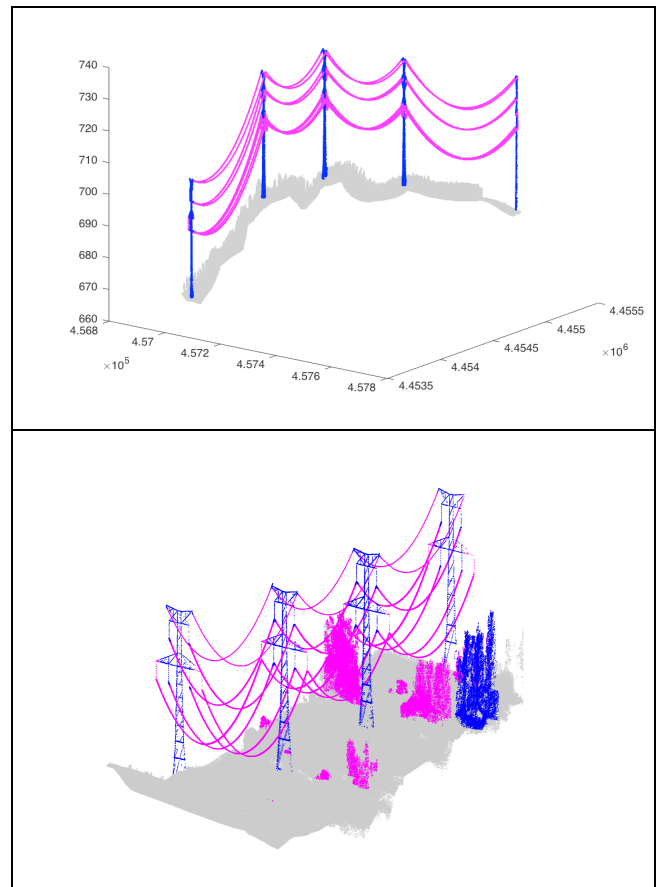


Figure 3 Initial classification for two files of the validation set. Subfigure on top presents a powerline over complex orography, while subfigure below presents trees near the powerline. Blue stands for pylon and magenta for wire areas.

The wire case has a special issue to take into account: there could be false positive points in correctly classified areas due to high vegetation or objects just below the wire itself. For this reason, the filtering process starts with the use of an agglomerative clustering algorithm [19] over all the candidate areas.

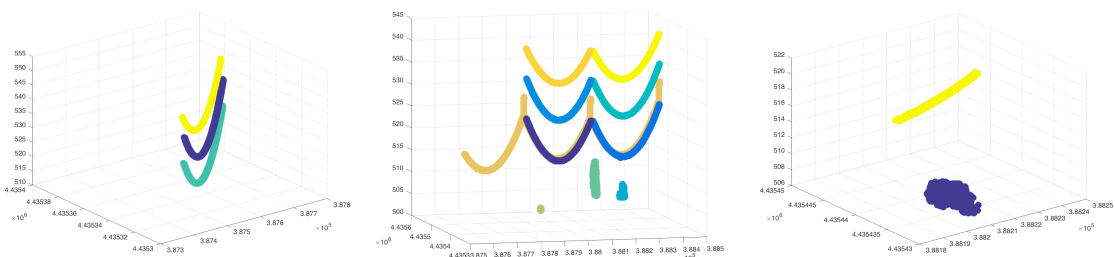


Figure 4: Agglomerative clustering applied to different wire candidate areas. Each cluster is represented with a different color. Subfigures in center and right include clusters with some small vegetation areas below the wires to be discarded.

The algorithm will join pairs of points or clusters step by step, choosing each time the closest pair based on a given distance, and stops when all possible distances between pairs are over a given cutoff. For this case, Euclidean distance between the positions of the points is used with a cutoff of 6. It is wide enough to differentiate wire clusters from possible vegetation areas near them, as it could be seen in the example of Figure 4.

Each cluster extracted by using the algorithm is then evaluated, confirming them as a wire if their intensity mean values remain below 2000, and removing it otherwise. All intensity thresholds during this stage have been set according to the initial analysis of data.

4. TEST CASES AND METHODOLOGY VALIDATION

In this section, two experiments are introduced to find the best configuration possible for the generation of images and validate the behavior of the method on a set with several different point clouds. A manual classification of the files is used as ground truth to compare.

All the experiments have been conducted in Matlab 2015b over a MacOS environment. From the four parameters given in the method, we provide the same values in every experiment for the following three: $\alpha = 1$, $\varepsilon = 8$, $\omega = 0.3$

4.1. Adjusting the γ parameter

As it has been explained in the methodology section, the generation of the binary image T for the selection of pylon candidate areas relies on a parameter, γ . We are looking for a value of γ which allows the classification of the maximum number of pylon points without generating a huge number of false positives to be corrected in the second stage. γ ranges between 0 and 1, so different values in this range have been tested over the validation set to generate T images. The second stage has not been executed during this experiment. The results can be found on Table 3.

From the results can be extracted that the use of low values of γ generates great amounts of false positives, although it also classifies the majority of pylon points. Increasing the value reduces drastically the number of false detections at expenses of a linear fall in the number of correctly classified points. $\gamma = 0.25$ seems to be a good value for the validation set when the goal is to classify as much points as

possible while controlling the referred errors in classification, and thus the execution time of the second stage.

γ	Detected	Non-detected	Falsely detected
0.15	255.2	11.6	205.1
0.20	252.1	14.8	100.3
0.25	249.4	17.5	66.9
0.30	245.1	21.7	52.5
0.35	241.8	25.0	45.5

Table 3 Results for pylon classification, using stage 1 over the validation set with different γ values. Numbers expressed in thousands of points.

	Validation set	Test set
<i>Point clouds size</i>	45502	44046
<i>Pylon: Ground Truth points</i>	266.8	262.6
<i>Pylon: well detected points</i>	249.4 (93.45% accuracy)	241.9 (92.14% accuracy)
<i>Pylon: non-detected points</i>	17.4 (6,55 %)	20.6 (7,86%)
<i>Pylon: false positives</i>	49.7 (0.11% of the set)	60.1 (0.14% of the set)
<i>Wire: Ground Truth points</i>	1695	1652
<i>Wire: well detected points</i>	1651 (97.37% accuracy)	1610 (97.44 % accuracy)
<i>Wire: non-detected points</i>	16.6 (2.63%)	42.3 (2.56%)
<i>Wire: false positives</i>	11.4 (0.03% of the set)	16.6 (0.04% of the set)
<i>Power line totals: Ground Truth</i>	1962	1915
<i>Power line totals: well detected</i>	1950 (99.37% accuracy)	1902 (99.33 % accuracy)
<i>Power line totals: non-detected</i>	12.4 (0.63%)	12.8 (0.67%)
<i>Power line totals: false positives</i>	11.5 (0.03% of the set)	26.5 (0.06% of the set)

Table 4 Results of the execution of the method over the validation and test sets. Numbers expressed in thousands of points.

4.2. Accuracy of the method

Our method was executed on the test set from Section 2, which includes 25 different point clouds

containing power lines and other elements. A run over the validation set was also conducted.

The results, which can be read in Table 4, show that the method generates promising results, with a 97,44 % of accuracy while classifying wires and a 92,14% of accuracy for pylon classification. According with these results, the method seems to be competitive compared with the reported results of other works: 97% and 92% respectively in the work of Kim and Sohn [12], 96,5% for wires from the work of Liang et al. [15] or 98,3% for wires from the work of Jwa et al. [11]. However, it is impossible to ensure it without a direct comparison of all the methods over the same point clouds. A final result for a given point cloud of the test result can be shown in Figure 5.

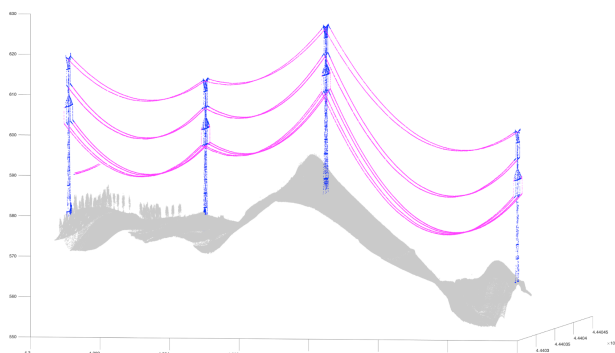


Figure 5 Final result of the classification process for a file of the test set.

On the other hand, there is still an appreciable number of false positives on pylon classification, of around 0,14% of the total size of the set. However, if both power line categories are considered as a single unit, the number of false positives is reduced to a 0,06%, which means much of the wrongly classified points in both wire and pylon groups belong to the other group. A future improvement to reclassify such points can increase the accuracy of the method and deal with the false positive issues at the same time.

5. CONCLUSIONS

In this paper, a method which classifies pylons and wires of power lines on discrete LiDAR point clouds is introduced. Our method avoids using a stage of preprocessing of ground points, which decreases the computational cost. Instead of that, binary images from all the available data to select the interesting points are generated. A second step groups the selected points with an agglomerative clustering algorithm and analyses the distribution of return values and the mean intensity of each cluster to discard false positives.

The results given by the method on a test set with 25 different point clouds are promising, with an accuracy of 97.44% for wire classification and 92.14% for pylon classification. Those results are similar to the ones reported in several reference studies.

The future lines of work will be focused on the refinement of the method, a more insightful study of performance and behavior, comparing with reference methods over the same scenarios, the extraction and 3D-modeling of single wires and pylons from the selected points and the detection of objects that could affect the power line.

ACKNOWLEDGEMENTS

The first author wants to thank Universidad de Las Palmas de Gran Canaria for its grant “Programa de personal investigador predoctoral en formación 2015”, which made possible this work.

REFERENCES

- [1] Lang, M., McCarty, G., Wilen, B., & Awl, J. (2010). Light Detection and Ranging. National Wetlands Newsletter, 32(5).
- [2] The American Society of Photogrammetry and Remote Sensing: Laser File Format Exchange Activities. Web Resource (last accessed 18.09.2017): <https://www.asprs.org/committee-general/laser-las-file-format-exchange-activities.html>
- [3] Brodu, N., & Lague, D. (2012). 3D terrestrial lidar data classification of complex natural scenes using a multi-scale dimensionality criterion: Applications in geomorphology. ISPRS Journal of Photogrammetry and Remote Sensing, 68, 121-134.
- [4] Antonarakis, A. S., Richards, K. S., & Brasington, J. (2008). Object-based land cover classification using airborne LiDAR. Remote Sensing of Environment, 112(6), 2988-2998.
- [5] Dalponte, M., Bruzzone, L., & Gianelle, D. (2008). Fusion of hyperspectral and LIDAR remote sensing data for classification of complex forest areas. IEEE Transactions on Geoscience and Remote Sensing, 46(5), 1416-1427.
- [6] Omar, A. H., Winker, D. M., Vaughan, M. A., Hu, Y., Trepte, C. R., Ferrare, R. A., ... & Kuehn, R. E. (2009). The CALIPSO automated aerosol classification and lidar ratio selection algorithm. Journal of Atmospheric and Oceanic Technology, 26(10), 1994-2014.

- [7] Niemeyer, J., Rottensteiner, F., & Soergel, U. (2014). Contextual classification of lidar data and building object detection in urban areas. *ISPRS journal of photogrammetry and remote sensing*, 87, 152-165.
- [8] Yao, W., Hinz, S., & Stilla, U. (2009, May). Object extraction based on 3d-segmentation of lidar data by combining mean shift with normalized cuts: Two examples from urban areas. In *Urban Remote Sensing Event, 2009 Joint* (pp. 1-6). IEEE.
- [9] Man, Q., Dong, P., & Guo, H. (2015). Pixel-and feature-level fusion of hyperspectral and lidar data for urban land-use classification. *International Journal of Remote Sensing*, 36(6), 1618-1644.
- [10] Liu, Y., Li, Z., Hayward, R., Walker, R., & Jin, H. (2009, December). Classification of airborne lidar intensity data using statistical analysis and hough transform with application to power line corridors. In *Digital Image Computing: Techniques and Applications, 2009. DICTA'09.* (pp. 462-467). IEEE.
- [11] Jwa, Y., Sohn, G., & Kim, H. B. (2009). Automatic 3d powerline reconstruction using airborne lidar data. *Int. Arch. Photogramm. Remote Sens*, 38(Part 3), W8.
- [12] Kim, H. B., & Sohn, G. (2010). 3D classification of power-line scene from airborne laser scanning data using random forests. *Int. Arch. Photogramm. Remote Sens*, 38, 126-132.
- [13] Kim, H. B., & Sohn, G. (2011). Random forests based multiple classifier system for power-line scene classification. *ISPRS Int. Arch. Photogramm., Remote Sens. Spat. Inf. Sci*, 253-258.
- [14] Zhu, L., & Hyyppä, J. (2014). Fully-automated power line extraction from airborne laser scanning point clouds in forest areas. *Remote Sensing*, 6(11), 11267-11282.
- [15] Liang, J., Zhang, J., Deng, K., Liu, Z., & Shi, Q. (2011, August). A new power-line extraction method based on airborne LiDAR point cloud data. In *Image and Data Fusion (ISIDF), 2011 International Symposium on* (pp. 1-4). IEEE.
- [16] Ritter, M., & Bengler, W. (2012). Reconstructing power cables from lidar data using eigenvector streamlines of the point distribution tensor field. *Journal of WSCG*.
- [17] Matikainen, L., Lehtomäki, M., Ahokas, E., Hyyppä, J., Karjalainen, M., Jaakkola, A., ... & Heinonen, T. (2016). Remote sensing methods for power line corridor surveys. *ISPRS Journal of Photogrammetry and Remote Sensing*, 119, 10-31.
- [18] Postes de alta y baja tensión. Web resource (last accessed 19.09.2017) : <https://electricidad-viatger.blogspot.com.es/2010/05/postes-de-alta-y-baja-tension-1.html>
- [19] Day, W. H., & Edelsbrunner, H. (1984). Efficient algorithms for agglomerative hierarchical clustering methods. *Journal of classification*, 1(1), 7-24.